J. Materials, Conc. Struct. Pavements, JSCE, No. 711/V-56, 205-215, 2002 August

SHEAR DEFORMATION OF REINFORCED CONCRETE BEAM

Tamon UEDA[1], Yasuhiko SATO[2], Tsunemasa ITO[3] and Katsuhide NISHIZONO[4]

[1]Member of JSCE, Dr. Eng., Associate Professor, Div. of Structural and Geotechnical Eng., Hokkaido University
(Nishi 8, Kita 13, Kita-ku, Sapporo 060-8628, Japan)
[2]Member of JSCE, Dr. Eng., Research Asociate, Div. of Structural and Geotechnical Eng., Hokkaido University
(Nishi 8, Kita 13, Kita-ku, Sapporo 060-8628, Japan)
[3]Member of JSCE, M. Eng., Engineer, 2nd Hokuriku Sinkansen Bureau, Japan Railway Construction Public Corporation
(Asahi-machi, Shimoshinkawa-gun, Toyama-ken, 939-0734, Japan)
[4]Member of JSCE, M. Eng., Engineer, Japan Bank for International Cooperation
(Otemachi 1-4-1, Chiyoda-ku, Tokyo 100-8144, Japan)

This paper presents the experimental results on shear deformation of concrete beams with shear reinforcement, which was measured by laser speckle method. The results indicate that besides flexural deformation the significant amount of shear deformation occurred after shear cracking, which was caused by the localized shear deformation along shear cracks. Based on the experimental results, a rather simple mechanical model for prediction of the deformation is proposed. The model consists of a truss model that calculates the shear deformation and a modified Branson's model with the tension shift concept to calculate the flexural deformation. The model can predict the experimental results well.

Key Words : *reinforced concrete beam, shear deformation, truss model, flexural deformation*

1. INTRODUCTION

Recently accurate prediction of deformations of reinforced concrete members has been considered more important because the performance-based design will be introduced as the next generation of design of structures. The performance-based design clearly specifies what are required performances of structures for serviceability, many of which are related to deformations of structures.

It is well known that flexural deformations of concrete members can be calculated with reasonable accuracy by the Branson's equation[1)], which is based on the Euler's beam theory. At the same time it is known that the Euler's theory, assuming that a plane in a beam remains after its flexural deformation, is no longer applicable after shear cracking[2)]. Neutral axis depths after shear cracking are smaller than those predicted by the Euler's beam theory.

It is considered that after shear cracking shear deformation is no longer negligible. However, there is no method commonly accepted for prediction of shear deformation. The truss theory that has been used for prediction of shear strength and shear reinforcement stress has been seldom used for prediction of deformation. One of the reasons of no method for shear deformation seems to be difficulty in measurement of shear deformation in experiment.

In this study the laser speckle method was applied to measure shear deformation of beams with shear reinforcement. Based on the experimental results a rather simple model to calculate deformation of beams was proposed. This model consists of a truss model for calculating shear deformation and a modified Branson's model for calculating flexural deformation. In the truss model tension stiffness of concrete surrounding shear reinforcement was considered. The influence of tension force increment in tension reinforcement induced by truss action after shear cracking, which is conventionally called moment shift, was considered in calculation of flexural deformation. In this paper, "moent sift" is called "tension shift".

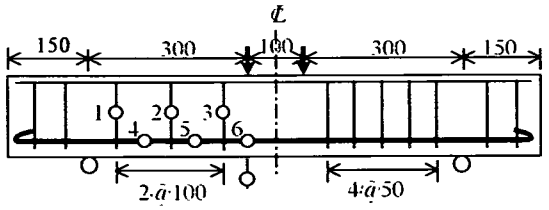

(a) Side view of specimens No.1 to No.4

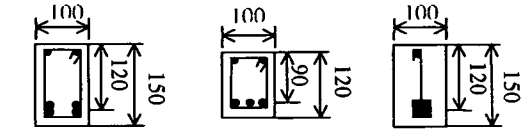

(b) Cross section of Specimens No.1 to No.4

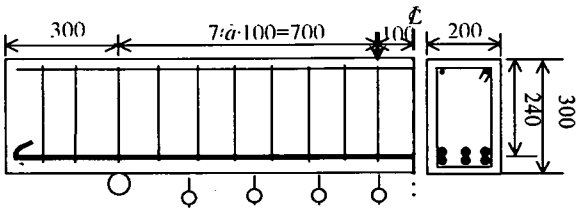

(c) Specimen No.5

Fig.1 Specimens

2. OUTLINE OF EXPERIMENT

In the experiment four small and one large beams with shear reinforcement were prepared. Experimental parameters are shear span to effective depth ratio, tension reinforcement ratio and shear reinforcement ratio. Details of the specimens are given in **Fig.1** and **Table 1**. Specimens No.1-4 are the small beams. Specimens 2, 3 and 4 are identical to specimen No.1, which is the reference beam, except for shear span to effective depth ratio (or effective depth), tension reinforcement ratio, and shear reinforcement ratio respectively. Specimen No.5 is the large beam. Concrete strength for each specimen is shown in **Table 1**. Maximum aggregate size of the concrete was 15 mm. Young's modulus and strengths of tension and shear reinforcement are shown in **Table 2**. High strength tension reinforcement was chosen for specimen No.3, so that flexural yielding would not happen.

Deflection at loading point was measured by displacement transducer for all the specimens and at additional 3 points in shear span for specimen No.5 (see **Fig.1 (c)**). Shear deformation in shear span in the small specimens (specimens No.1-4) was measured by the laser speckle method[3]. The laser speckle method is an optical measuring method for in-plane displacement.

Table 1 Specimens and test results

Specimen	f_c' (MPa)	a/d	p_s (%)	p_w (%)	V_u (kN)
No.1	40.2	2.5	4.22	0.63	67
No.2	54.7	3.3	4.22	0.63	39
No.3	41.0	2.5	2.38	0.63	60
No.4	40.5	2.5	4.22	0.32	48
No.5	31.7	2.92	4.46	0.72	235

1) f_c' : concrete strength, a/d : shear span to depth ratio, p_s : tension reinforcement ratio. p_w : shear reinforcement ratio, and V_u : ultimate strength

Table 2 Material properties of reinforcement

Type	A_s (mm²)	f_y (MPa)	E_s (GPa)
D6	31.67	355	183
D10	71.33	791	197
D13	126.7	355	170
D22	387.1	392	178

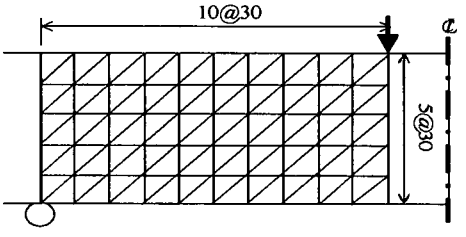

Fig.2 Measuring points for laser speckle method (specimens No.1, 3, and 4)

Movement in any direction of any point in a target area can be measured with accuracy of 1 μ m order. Size of target area depends on capacity of laser beam. In this test it was approximately 300 x 300 mm. This is the reason why shear span was chosen to be 300 mm for the small specimens. Movements of sixty-six nodes (fifty-five nodes for specimen No.2) in **Fig.2** were measured by the laser speckle method to calculate strains, ε_x, ε_y and γ_{xy} of 100 triangle elements (80 elements for specimen No.2). The strains of upper triangles were calculated using the nodal movements, u and v as follows:

$$\varepsilon_x = (u_j - u_i)/\Delta x \tag{1a}$$

$$\varepsilon_y = (v_k - v_i)/\Delta y \tag{1b}$$

$$\gamma_{xy} = (u_k - u_i)/\Delta x + (v_j - v_i)/\Delta y \tag{1c}$$

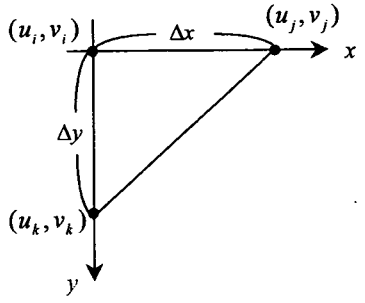

Fig.3 Grid for calculation of strain

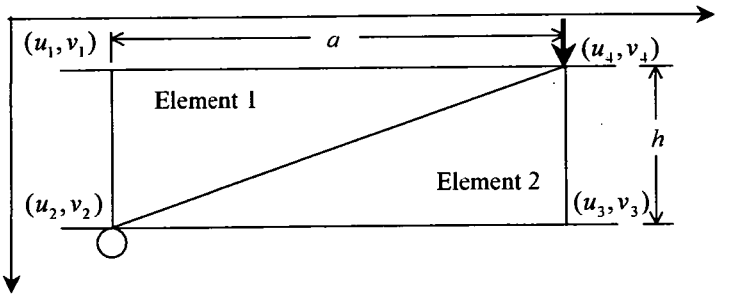

Fig.4 Calculation of shear deformation

where explanation for the notation can be seen in **Fig.3**. Strains for lower triangles can be calculated by a similar way. Location of neutral axis was obtained from distribution of ε_x. Shear deformation of the specimen, δ_s was calculated as average shear strain in shear span multiplied by shear span length, a as follows:

$$\delta_s = \bar{\gamma}_{xy} a = \frac{\gamma_{xy1} + \gamma_{xy2}}{2} a \tag{2}$$

where $\gamma_{xy1} = (u_2 - u_1)/h + (v_4 - v_1)/a$ (3a)

$$\gamma_{xy2} = -(u_4 - u_3)/h - (v_2 - v_3)/a \tag{3b}$$

Notations in the above equations are as shown in **Fig.4**. Flexural deformation of the specimen, δ_f was calculated by subtracting shear deformation from deflection at loading point, δ, namely:

$$\delta_f = \delta - \delta_s \tag{4}$$

Strains of the tension reinforcement were measured at maximum moment region and points between shear reinforcement (see **Fig.1 (a)**). Strains were measured at one point of each shear reinforcement in the small specimens and at two points of each shear reinforcement in the large specimen.

Load was monotonically increased with a displacement increment of 200m at the loading point until the specimens failed.

3. EXPERIMENTAL RESULTS

(1) Failure characteristics

Specimen No.1 failed in flexure with yielding of tension reinforcement, while the other specimens showed shear failure without yielding of the tension reinforcement.

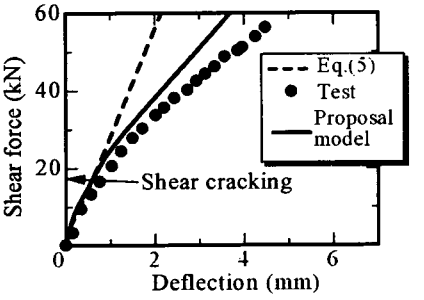

Fig.5 Relationships between applied shear force and total deformation for specimen No.3

(2) Deformation characteristics

Relationship between applied shear force and deflection at loading point in specimen No.2 is shown in **Fig.5**. It is seen that deflection at the loading point before shear cracking can be predicted by the following equation that is derived from the Euler's beam theory in which the Branson's equation for effective moment of inertia is applied:

$$\delta_f = \frac{Va^3}{6E_c I_e}\left\{-x^3 + 3a(a+2c)x\right\} \tag{5}$$

where V is applied shear force, E_c is Young's modulus of concrete, x is distance from support to point considered ($0 \le x \le a$), a is shear span, c is a half of distance between two loading points, and I_e is effective moment of inertia that can be calculated as follows:

$$I_e = I_g\left(\frac{M_{cr}}{M_{\max}}\right)^3 + I_{cr}\left\{1 - \left(\frac{M_{cr}}{M_{\max}}\right)^3\right\} \tag{6}$$

where I_g and I_{cr} are moment of inertia of concrete gross and cracked section, M_{cr} and $M_{\max}$ are cracking and maximum moment at loading point under applied shear force, V. It can be said, therefore, that before shear cracking deformation is mostly flexural deformation.

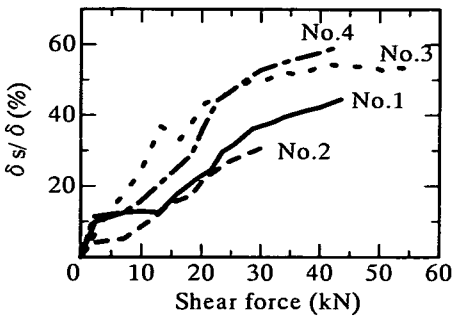

Fig.6 Ratio of shear deformation to total deformation

However, observed deflection is significantly greater than that calculated by the Branson's equation after shear cracking. There is effect of shear cracking.

Ratio of shear deformation to total deformation (δ_s/δ) for the smaller specimen is shown in **Fig.6**. The shear deformation is calculated by Eq.(2). The ratio is larger for specimen with smaller shear span to effective depth ratio, smaller tension reinforcement ratio and smaller shear reinforcement ratio.

(3) Concrete strain characteristics

Cracking pattern observed in specimen No.1 is shown in **Fig.7**. Its distribution of shear strain, which is calculated as average of shear strains in a pair of an upper and a lower triangle element (see **Figs. 2** and **3**), is shown in **Fig.8**. Distribution of corresponding principal strains is shown in **Fig.9**. It can be said that after shear cracking took place at 22 kN large and localized shear strains are seen along the shear crack. Normal strain distribution in specimen No.1 is indicated in **Fig.10**. It is clearly seen that observed neutral axis depth indicated by solid lines is smaller than that predicted in an Euler's beam with no concrete stress in tension (see broken lines in the figure).

(4) Reinforcement strain characteristics

Relationship between applied shear force and strain in tension reinforcement in specimen No.4 is shown in **Fig.11**. The strain in tension reinforcement at point 4 (see **Fig.1 (a)**) increases more quickly and becomes larger than the one predicted by the Euler's beam theory with stiffness of cracked section. This quicker increase can be explained by so called "moment shift". Moment shift is explained by truss action in which horizontal component of force in diagonal compression strut is balanced with force in tension chord (tension reinforcement). Since diagonal strut does not exist in beam action, additional force would act in tension reinforcement once truss action starts to work.

Strain in shear reinforcement of specimen No.3 is shown as relationship with applied shear force in

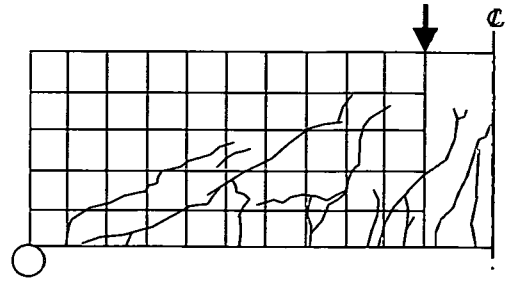

Fig.7 Cracking pattern in specimen No.1

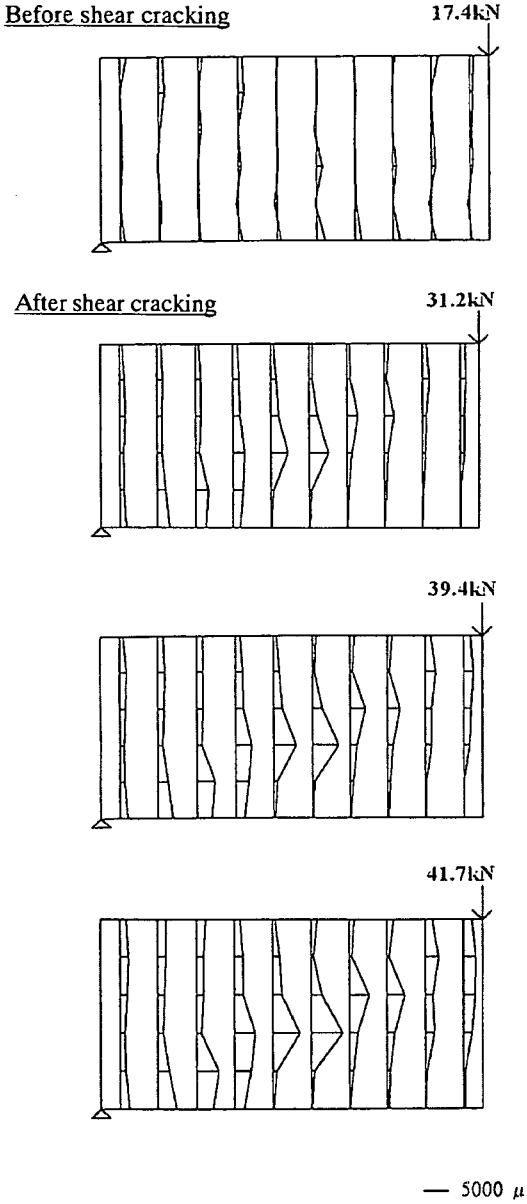

Fig.8 Concrete shear strain distribution for specimen No.1

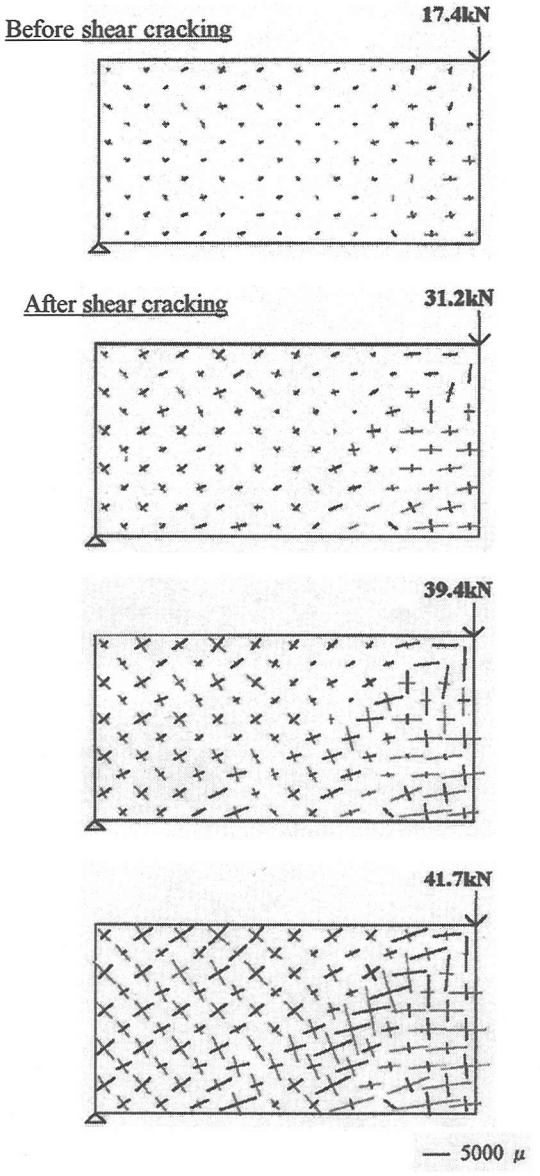

Fig.9 Principal strain distribution for specimen No.1

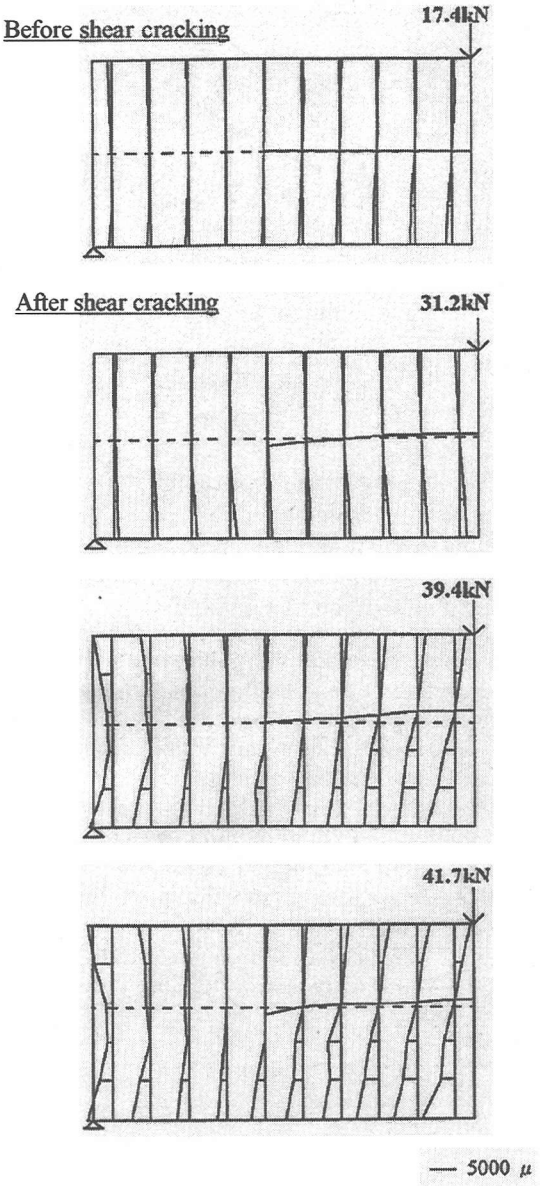

Fig.10 Normal strain in direction of member axis and neutral axis for specimen No.1

Fig.12.Measuring point is point 3 shown in **Fig.1 (a)**. It is known that relationship between applied shear orce, V and strain in shear reinforcement, ε_w can be expressed by truss action as follows:

$$V = V_c + V_s = V_c + A_w E_w \varepsilon_w (\cot\alpha + \cot\theta) z/s \quad (7)$$

where V_c is applied shear force at shear cracking, V_s is shear force carried by truss mechanism, A_w is cross sectional area of shear reinforcement within spacing, s, E_w and α are Young's modulus and angle with member axis of shear reinforcement, θ is angle of compression diagonal strut, and z is distance between centroids of forces in compression and tension chord. The observed strain in **Fig.12** is much smaller than that predicted by Eq.(7).

4. PROPOSED MODEL FOR SHEAR DEFORMATION

In this section proposed model for calculation of shear deformation before and after flexural and shear cracking of beams is presented. Shear deformation in this paper includes additional flexural deformation due to shear cracking.

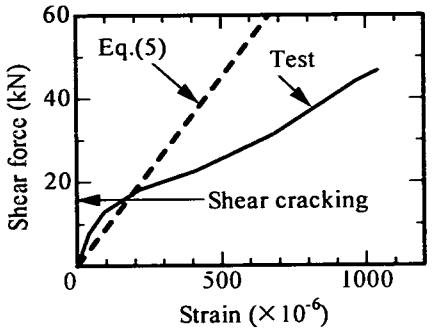

Fig.11 Relationships between applied shear force and strain in tension reinforcement (specimen No.4)

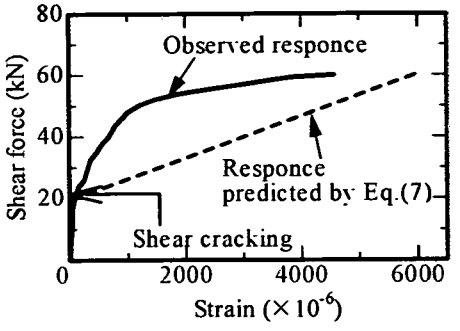

Fig.12 Relationships between applied shear force and strain in shear reinforcement (specimen No.3)

(1)Model for additional flexural deformation due to shear cracking

It is considered that the Branson's method can be used to calculate flexural deformation with consideration of tension force increase in tension reinforcement induced by truss action occurring after shear cracking (see **Fig.11**). Since tension force in tension reinforcement actually changes instead of moment acting on beam, a new terminology, "tension shift" instead of "moment shift" is used in this study.

Amount of "tension shift", ΔT can be calculated from truss mechanism which carries a part of total shear force, V_s. For this purpose a free body of the truss mechanism is considered as shown in **Fig.13**. The line CD is in parallel to the diagonal compression strut whose angle with the member axis is θ. From the equilibrium between tension force across the line CD, $T_{st,t}$ and V_s, the following equation is derived:

$$T_{st,t} = \frac{V_s}{\sin\alpha} \tag{8}$$

where α is angle of shear reinforcement with member axis. The equilibrium for moment around point D induced by tension force in the tension chord, T_c, and is

$$V_s(x + z\cot\theta) - T_c z - \frac{1}{2}\frac{z}{\sin\theta}\sin(\theta+\alpha)T_{st,t} = 0 \tag{9}$$

where x is the distance of point C from support. Substituting Eq.(8) in Eq.(9), the following equation is then obtained:

$$T_c = \left[\frac{x}{z} + \cot\theta - \frac{\sin(\theta+\alpha)}{2\sin\theta\sin\alpha}\right]V_s \tag{10}$$

If it is assumed that beam action carries the total shear force subtracted by the shear force carried by truss mechanism, $V - V_s$, tension force in the tension reinforcement (or the tension chord in truss) at point C

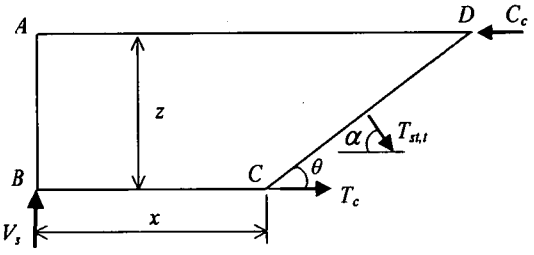

Fig.13 Free body for calculation of tension shift, ΔT

is

$$T_b = \frac{x}{z}(V - V_s) \tag{11}$$

On the other hand, if beam action carries all the shear force, tension force in the tension reinforcement at point C is

$$T = \frac{x}{z}V \tag{12}$$

From Eqs.(10), (11) and (12), the amount of tension shift, ΔT that is the tension force increase in the tension reinforcement is as follows:

$$\Delta T = T_c + T_b - T = \left[\cot\theta - \frac{\sin(\theta+\alpha)}{2\sin\theta\sin\alpha}\right]V_s \tag{13}$$

However, total tension force in tension reinforcement never goes beyond the maximum tension force induced by moment. Additional flexural deformation due to "tension shift" is calculated by assuming that "tension shift" creates additional deformation whose amount is the same as that caused by moment inducing the same amount of tension force in tension reinforcement. This

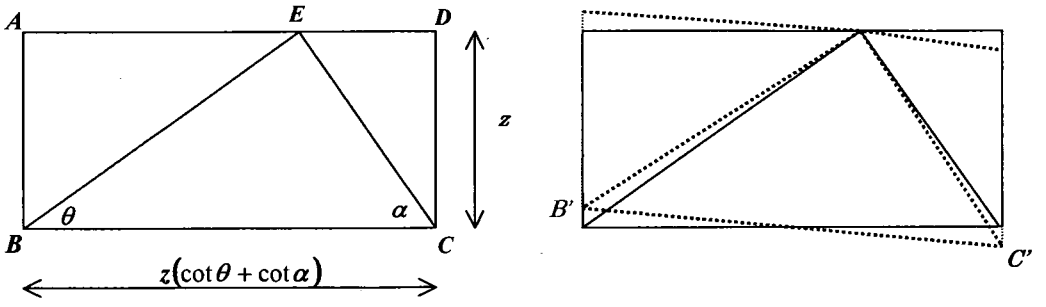

(a) Assumed truss unit (b) Deformation of truss unit

Fig.14 Truss unit for calculation of shear deformation

assumption is in fact conservative. The reason is as follows. Actually additional deformation due to increase in moment in beam action is different from that due to tension shift in truss mechanism. The moment increase causes increase in elongation in tension zone and contraction in compression zone, while the tension shift increases elongation in both tension and compression chord of truss mechanism. The elongation of tension chord is much greater than that of compression chord because the tension chord is cracked concrete (or tension reinforcement) and the compression chord is uncracked concrete. This difference in elongation induces additional flexural deformation, which is smaller than that induced by increase in moment in beam action.

(2) Model for shear deformation before shear cracking

It is assumed that shear deformation before shear cracking can be calculated by elastic theory for beam as follows:

$$\delta_s = \kappa \int \frac{V}{G_c A_e} dx \tag{14}$$

where $\kappa = 6/5$ for rectangular section. G_c is shear stiffness of concrete ($= E_c / [2(1+\nu_c)]$), ν_c is Poisson's ratio of concrete, and A_e is concrete effective cross-sectional area, which is calculated as follows:

before flexural cracking,

$$A_e = A_g \tag{15a}$$

after flexural cracking,

$$A_e = A_g \left(\frac{M_{cr}}{M_{\max}} \right)^3 + A_{cr} \left[1 - \left(\frac{M_{cr}}{M_{\max}} \right)^3 \right] \tag{15b}$$

where A_g is concrete gross section ($= bh$ for rectangular section), b and h are width and height of cross section, n is Young's modulus ratio ($= E_s / E_c$) and A_{cr} is cross-sectional area of cracked section. Equation (15b) is introduced by assuming that effective concrete area for shear stiffness be reduced due to flexural cracking.

Although Eqs.(14) and (15) are proposed, experimental facts indicate that shear deformation is usually much smaller than flexural deformation and can be neglected.

(3) Shear deformation after shear cracking

After shear cracking, it is assumed that shear deformation is caused by truss mechanism. Since deformation of truss due to deformation of tension and compression chord is considered in flexural deformation, truss deformation due to deformation of tie and compression strut is considered as shear deformation. Let's consider a truss unit $ABCD$ consisting of tie and compression strut with horizontal size of $z(\cot\theta + \cot\alpha)$ and vertical size of z as shown in **Fig.14**. The truss unit is a part of a beam where shear cracks exist. Line BE is in parallel to compression strut whose angle to tension chord (or tension reinforcement) is θ. Line CE is in parallel to tie whose angle is α. Cross-sectional areas of the compression strut crossing line is as follows:

$$A_{st,c} = b_w z(\cot\theta + \cot\alpha)\sin\theta \tag{16}$$

When applied shear force on the truss mechanism is V_s, stress acting in compression strut is calculated by equilibrium as follows:

$$\sigma'_{st,c} = \frac{V_s}{A_{st,c}\sin\theta} = \frac{V_s}{b_w z(\cot\theta + \cot\alpha)\sin^2\theta} \tag{17}$$

Thus strain in compression strut is

$$\varepsilon'_{st,c} = \frac{\sigma'_{st,c}}{E_c} \tag{18}$$

Since the length of compression strut is

$$l_{st,c} = \frac{z}{\sin\theta} \tag{19}$$

deformation (shortening) of the compression strut is

$$\Delta l_{st,c} = l_{st,c}\varepsilon'_{st,c} = \frac{V_s}{E_c b_w (\cot\theta + \cot\alpha)\sin^3\theta} \tag{20}$$

This deformation moves point B to B' in **Fig.14**. The vertical component of the movement of point that indicates shear deformation induced by deformation of compression strut is expressed by the following equation:

$$\delta_{s1} = \frac{\Delta l_{st,c}}{\sin\theta} = \frac{V_s}{E_c b_w (\cot\theta + \cot\alpha)\sin^4\theta} \tag{21}$$

Similarly shear deformation due to deformation of tie can be calculated. Cross-sectional area of tie that consists of shear reinforcement and its surrounding concrete effective in tension is assumed to be

$$A_{st,to} = A_w + \frac{E_c}{E_w} A_{ce} \tag{22}$$

with $A_{ce} = A_{ceo}(V_c/V)^3$ (23)

where A_w is cross-sectional area of shear reinforcement in a spacing, s, A_{ce} is cross-sectional area of surrounding concrete effective in tension, and A_{ceo} is A_{ce} immediate after shear cracking and can be calculated by the method proposed by An et al[5]. Number of shear reinforcement crossing line is

$$n_w = \frac{z(\cot\theta + \cot\alpha)}{s} \tag{24}$$

Cross-sectional area of tie, crossing line BE is

$$A_{st,t} = \frac{z(\cot\theta + \cot\alpha)}{s}\left(A_w + \frac{E_c}{E_w} A_{ce}\right) \tag{25}$$

Stress in the tie can be calculated by equilibrium as follows:

$$\sigma_{st,t} = \frac{V_s}{A_{st,t}\sin\alpha} = \frac{V_s s}{\left(A_w + \frac{E_c}{E_w} A_{ce}\right) z(\cot\theta + \cot\alpha)\sin\alpha} \tag{26}$$

Strain in the tie is then

$$\varepsilon_{st,t} = \frac{\sigma_{st,t}}{E_w} \tag{27}$$

Since length of tie is

$$l_{st,t} = \frac{z}{\sin\alpha} \tag{28}$$

deformation (elongation) of the tie is

$$\Delta l_{st,t} = l_{st,t}\varepsilon_{st,t} = \frac{V_s s}{E_w\left(A_w + \frac{E_c}{E_w} A_{ce}\right)(\cot\theta + \cot\alpha)\sin^2\alpha} \tag{29}$$

Due to this deformation, point C moves to C' in **Fig.14**. Vertical component of the movement, which is a part of shear deformation, is expressed by the following equation:

$$\delta_{s2} = \frac{\Delta l_{st,t}}{\sin\alpha} = \frac{V_s s}{E_w\left(A_w + \frac{E_c}{E_w} A_{ce}\right)(\cot\theta + \cot\alpha)\sin^3\alpha} \tag{30}$$

Consequently shear deformation of the truss unit shown in **Fig.13** is calculated from Eqs.(21) and (30) as follows:

$$\delta_s = \delta_{s1} + \delta_{s2} \tag{31}$$

Its corresponding shear strain is

$$\gamma = \frac{\delta_s}{z(\cot\theta + \cot\alpha)} \tag{32}$$

Finally shear deformation of a beam can be calculated by integrating shear strain as follows:

$$\delta_s = \int \gamma dx = \int \frac{1}{z(\cot\theta + \cot\alpha)^2}\left[\frac{V_s}{E_c b_w \sin^4\theta} + \frac{V_s s}{E_w\left(A_w + \frac{E_c}{E_w} A_{ce}\right)\sin^3\alpha}\right] dx \tag{33}$$

The angle for tie, α is given as an angle of shear reinforcement with member axis. However, the angle

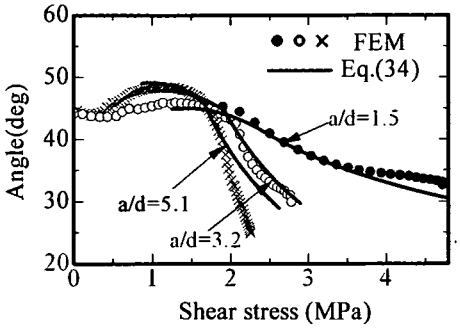

Fig.15 Angle of compression strut

for compression strut, θ has to be given based on actual compression stress flow in concrete. In this study numerical experiment with nonlinear finite element program[4] was conducted to find θ. **Figure 15** shows the variation of θ, which was found to increase slightly before shear cracking and decrease gradually after shear cracking. It was also found that the θ variation was influenced by some factors such as shear span to depth ratio, tension reinforcement ratio and shear reinforcement ratio. As a result, the following equation was proposed to evaluate the θ variation with reasonable accuracy (see **Fig.15**):

$$\theta = -\alpha(v - v_0)^2 + \theta_0 \quad \text{for } v_0 \le v < 1.7v_c \qquad (34a)$$

$$\theta = \theta_1\left(\frac{1.7v_0}{v}\right)^{\beta} \quad \text{for } 1.7v_c \le v \qquad (34b)$$

with $\theta_0 = 3.2\left(\frac{a}{d}\right) + 40.2$ for $a/d > 1.5$ (35)

$$\theta_1 = -\alpha(1.7v_c - v_0)^2 + \theta_0 \qquad (36)$$

$$v_0 = 0.9v_c \qquad (37)$$

$$v_c = 0.2f_c'^{1/3}(100p_t)^{1/3}(1/d)^{1/4}\left(0.75 + \frac{1.4}{a/d}\right) \qquad (38)$$

$$\alpha = 0.4\left(\frac{a}{d}\right)^2 + 2.9 \qquad (39)$$

$$\beta = (0.7 - 32\sqrt{p_t p_w})\frac{a}{d} \qquad (40)$$

where v is nominal shear stress ($=V/(bd)$), v_c is nominal shear stress at shear cracking, p_t is tension reinforcement ratio, p_w is shear reinforcement ratio, and a/d is shear span to depth ratio (>1.5).

Consequently shear deformation after shear cracking is summation of the shear deformation of the truss calculated by Eq.(33) and the shear deformation right before shear cracking calculated by Eq.(40).

$$\delta_{sc} = k\int\frac{2V_c}{GA_e}dx \qquad (40)$$

Because of its nature Eq.(33) for calculation of shear deformation can be applied to not only the case of point loading but also distributed loading. In the latter case the shear force carried by the truss mechanism, or $V - V_c$ is varying for different x.

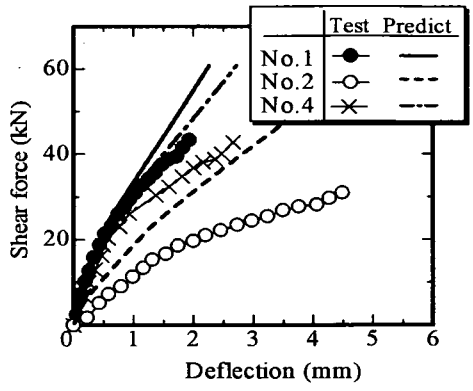

(a) Specimens No.1, No.2 and No.4

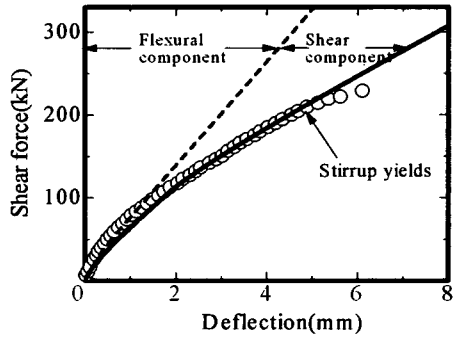

(b) Specimen No.5

Fig.16 Comparison of predicted deformation with observed deformation

(4) Verification of proposed model

Figure 16 shows comparison between experimental and calculated load-deformation curves of specimens No.1, No.2, No.4 and No.5. A result of specimen No.3 is shown in Fig.5. As seen in **Fig.16(b)** the calculated flexural deformation significantly underestimates the

Table 3 Test specimens in Ref.(6)

Specimen	f_c' (MPa)	a/d	p_s (%)	p_w (%)
A-1	24	3.92	1.8	1.0
A-2	24	4.93	2.3	1.0
A-3	35	6.91	2.7	1.0
B-1	25	3.95	2.4	0.8
B-2	23	4.91	2.4	1.5
B-3	39	6.95	3.1	1.5
C-1	30	3.95	1.8	2.0
C-2	24	4.93	3.7	2.0
C-3	35	6.98	3.6	2.0

experimental deformation after shear cracking. The proposed model can simulate the experimental results reasonably for specimens No.1, No.3 and No.5. In specimen No.2 the observed deformation is larger than calculated one from the early stage because displacement at supporting points could not be measured correctly. It could be considered in specimen No.4 that slippage of stirrup at the hook (see **Fig.1**) have produced the unexpected deformation.

Figure 17 shows comparison with previous study[6] in which the tension and shear reinforcement ratios, and *a/d* are varied from 1.8 to 3.7%, 0.8 to 2%, and 3.92 to 6.98, respectively (see **Table 3**). It can be said that the proposed model can predict the experimental results with good accuracy except for higher load level in some specimen with smaller *a/d* ratios. The discrepancy in the higher load level observed in specimens A-1, A-2, B-1, and B-2 may be caused by yielding of stirrups. Unfortunately no information on the yielding is given in the reference.

The proposed model will be extended to the model which can consider the yielding of reinforcing bars.

5. CONCLUSIONS

(1)Two-dimensional distribution of shear strain in shear span was measured by an optical measuring method (laser speckle method). It was observed that shear strain was rather localized along shear crack.

(2) Significant shear deformation was observed in the experiment after shear cracking.

(3) Due to the shear deformation conventional method for prediction of flexural deformation (Branson's method) underestimates the observed deformation significantly.

(4) Methods to calculate additional flexural deformation due to tension shift induced by shear cracking and to calculate shear deformation were presented.

(5) The prediction method for shear deformation that is based on truss mechanism can be applied to not only point loading but also distributed loading.

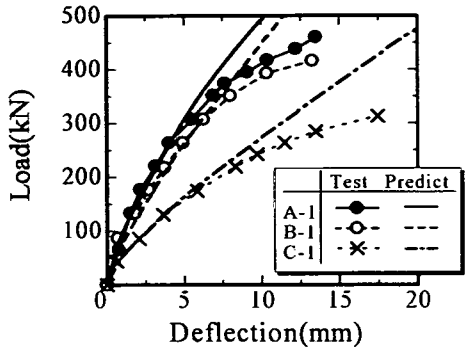

(a) *a/d* is about 4.0

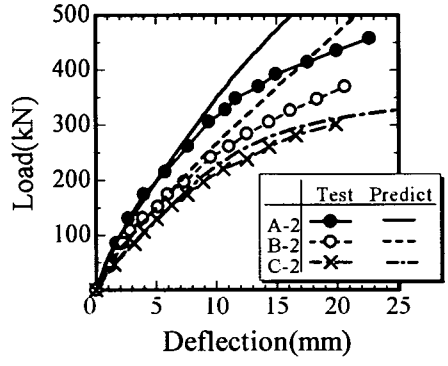

(b) *a/d* is about 5.0

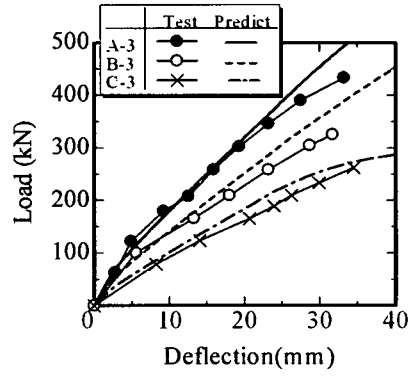

(c) *a/d* is about 7.0

Fig.17 Comparison with experimental results reported in Ref.(6)

(6)The proposed methods predict the observed deformation with reasonable accuracy.

ACKNOWLEDGMENT: The authors would like to express their sincere gratitude to Prof KAKUTA Yoshio and Prof Takahashi Yoshihiro for their valuable advice to this study and Mr KIMURA Tsutomu for his assistance to the experiment in this study.

REFERENCES

1) Branson, D. E. and Trost, H.: Unified procedures for predicting the deformation and centroidal axis location of partially cracked nonprestressed and prestressed concrete members, *ACI J.*, Vol.79, No.2, pp.119-128, 1982.
2) Sato, Y., Ueda, T. and Kakuta, Y.: Qualitative evaluation of shear resisting behavior of concrete beams reinforced with FRP rods by finite element analysis", *Concrete Library International*, JSCE, No.24, pp.193-209, 1994.
3) Pallewatta, T. M., Tada, H. and Horii, H.: Measurement of displacement field of concrete by laser speckle method, *Transaction of JCI*, Vol.12, No.1, pp.835-840, 1990.
4) Ueda, T., Pantaratorn, N. and Sato, Y.: Finite element analysis on shear resisting mechanism of concrete beams with shear reinforcement", *Journal of Materials, Concrete Structures and Pavements*, JSCE, No.520/V-28, pp.273-286, August 1995.
5) An, X., Maekawa, K. and Okamura, H.: Numerical simulation of size effect in shear strength of RC beams, *Concrete Library of JSCE*, NO. 31, pp. 323-346, June 1998.

(Received September 26, 2001)

鉄筋コンクリート棒部材のせん断変形

上田多門・佐藤靖彦・伊藤常正・西園勝秀

本論文では，光学的手法であるレーザースペックル法によって測定された，せん断補強筋を有するはりのせん断変形の実験結果を示している．それによれば，曲げ変形に加え，無視できないほどの大きさのせん断変形が，せん断ひび割れ部に集中して生じた局部的なせん断変形により，生じていた．実験結果に基づき，変形を推定するための簡便な力学モデルを提案している．提案モデルは，せん断変形を算定するためのトラスモデルと，テンションシフトによる付加的な曲げ変形を算定するためのモデルとからなっている．モデルは，実験結果を精度よく推定できている．